
LUGo: AN ENHANCED QUANTUM PHASE ESTIMATION IMPLEMENTATION

A PREPRINT

Chao Lu^{a,†}, Muralikrishnan Gopalakrishnan Meena^a, and Kalyana C. Gottiparthi^a

^aNational Center for Computational Sciences, Oak Ridge National Laboratory, Oak Ridge, TN, USA

[†]To whom correspondence should be addressed: luc1@ornl.gov

March 20, 2025

ABSTRACT

Quantum Phase Estimation (QPE) is a cardinal algorithm in quantum computing that plays a crucial role in various applications, including cryptography, molecular simulation, and solving systems of linear equations. However, the standard implementation of QPE faces challenges related to time complexity and circuit depth, which limit its practicality for large-scale computations. We introduce LuGo, a novel framework designed to enhance the performance of QPE by reducing redundant circuit duplication, as well as parallelization techniques to achieve faster circuit generation and gate reduction. We validate the effectiveness of our framework by generating quantum linear solver circuits, which require both QPE and inverse QPE, to solve linear systems of equations. LuGo achieves significant improvements in both computational efficiency and hardware requirements while maintaining high accuracy. Compared to a standard QPE implementation, LuGo reduces time consumption to solve a $2^6 \times 2^6$ system matrix by a factor of 50.68 and over $31\times$ reduction of quantum gates and circuit depth, with no fidelity loss on an ideal quantum simulator. With these advantages, LuGo paves the way for more efficient implementations of QPE, enabling broader applications across several quantum computing domains. ¹

1 Introduction

Quantum computing has demonstrated significant promise through advancements in algorithms and hardware. Leading technology companies are exploring diverse approaches to develop robust, large-scale quantum computers capable of implementing these algorithms. Notably, IBM now provides public access to superconducting quantum computers with over 150 qubits via its cloud platform [1]. Google’s Sycamore quantum chip has successfully implemented an efficient quantum error-correction code, achieving an error rate below 10^{-6} [2]. Quantum algorithms are proving to offer exponential speedups over their classical counterparts in areas such as machine learning, cryptography, quantum physics, and fluid dynamics [3–11].

However, considerable efforts are still needed to enable quantum computers to effectively address real-world problems. In parallel, the development of quantum algorithms remains critical for efficient design and implementation. Several groundbreaking algorithms, including Shor’s algorithm, Grover’s search algorithm, the Quantum Approximate Optimization Algorithm (QAOA), the Quantum Linear Systems Algorithm (QLSA), and the Quantum Phase Estimation (QPE) algorithm have been proposed to tackle computational challenges that are infeasible for classical systems [12, 13]. Despite their theoretical potential for exponential acceleration, the practical implementation and scalability of many of these algorithms face significant hurdles.

¹**Notice:** This manuscript has been authored by UT-Battelle, LLC, under contract DE-AC05-00OR22725 with the US Department of Energy (DOE). The US government retains and the publisher, by accepting the article for publication, acknowledges that the US government retains a nonexclusive, paid-up, irrevocable, worldwide license to publish or reproduce the published form of this manuscript, or allow others to do so, for US government purposes. DOE will provide public access to these results of federally sponsored research in accordance with the DOE Public Access Plan (<http://energy.gov/downloads/doe-public-access-plan>).

Quantum Phase Estimation (QPE), as a fundamental algorithm in quantum computing, serves as a cornerstone for various applications. It was first introduced in 1995 to estimate the phase of a unitary matrix [14]. Over the years, numerous studies have focused on enhancing the implementation and optimization of QPE to improve its efficiency and scalability. Among these, QPE stands out for its versatility in solving problems with exponential speedups. As one of the cornerstone algorithms in quantum computation, QPE has already been integrated in several quantum software development kits [1, 15–18]. However, QPE faces several challenges, including generating controlled-unitary circuits, which are critical to its functionality. Optimizing QPE design is crucial to improve the performance of various quantum algorithms that rely on it [12]. Moreover, maintaining high fidelity while executing QPE on real quantum hardware remains difficult.

Several directions of improving fidelity of QPE have been attempted for more robust and efficient implementation. An evolutionary algorithm was applied to reduce the fidelity loss due to Trotter Approximation for QPE algorithm [19]. Kang et al. optimized QPE algorithm specifically for simulating electronic states, introducing ‘QPESIM’ for the simulation [20]. Iterative QPE implementations have also been explored for better precision [21–23]. Li proposed an iterative QPE implementation for precise readout on noisy intermediate-scale quantum (NISQ) devices with only a few ancilla qubits [24]. Van et al. improved iterative QPE algorithm for optimized sample complexity, enabling minimal sampling size required for acceptable accuracy [23]. [22] proposed an iterative QPE for reduced circuit implementation. Mohammadbagherpoor et al. improved QPE circuits by removing unnecessary controlled unitary gates and replaced with unitary operators [25]. However, such implementations are applicable only in limited scenarios where the controlled unitary operators can be replaced. Others, use alternative approaches to replace part of the QPE algorithm, where it either does not generalize well to most quantum hardware [26], reduce accuracy [27], or require additional circuit complexity [28].

To extend the capability of quantum algorithms that depends on QPE, improving QPE is an opportunity to pave the way for practical quantum computing solutions that could redefine our understanding of the world and solve problems once thought insurmountable. In this paper, we introduce LuGo, a QPE circuit design aiming for a scalable and efficient quantum circuit generation. We demonstrate the capability of LuGo on a quantum linear solver algorithm (QLSA), the Harrow–Hassidim–Lloyd (HHL) algorithm [29]. The major contribution of the paper are:

- We introduce LuGo, a new Quantum Phase Estimation (QPE) circuits generation approach.
- We implemented LuGo on HHL algorithm that utilize QPE as a sub-algorithm to illustrate the efficiency of LuGo.
- LuGo achieves the time consumption reduction by $50.68\times$ and over $31\times$ on circuit depth and gate reduction on $2^6 \times 2^6$ matrix input on generated HHL circuits without fidelity loss.
- We validate and benchmark the new HHL circuit generation algorithm on the Frontier supercomputer to analyze the scalability and fidelity of the proposed LuGo framework.

The rest of this paper is organized as follows. We first provide the results in Section 2: performance comparison of LuGo and standard QPE with respect to time consumption, circuit statistics, and fidelity as integrated in HHL circuits and run on ideal quantum simulator. Section 3 provides background on the methods and algorithms, including the QPE algorithm, the Peter–Weyl decomposition algorithm that is used for the generation of unitary circuits for QPE, and the proposed LuGo framework. We provide some discussion and final remarks in Section 4.

2 Results

In this section, we evaluate the performance of our LuGo framework compared with the standard QPE circuit generation approach. The QPE implementations are demonstrated on the HHL algorithm [29], a canonical QLSA algorithm. All developments are performed using Qiskit (version 1.3) [1]. We utilize tridiagonal Toeplitz matrices as the linear systems of equations to benchmark the two QPE circuits generation algorithm. However, LuGo and standard QPE can take any arbitrary unitary matrix as the input to solve linear systems of equations, and any matrix can be transformed to a unitary matrix as discussed in Section 3.2. Details of the standard QPE and LuGo methods are described in Section 3.

To measure execution time, we used the Oak Ridge Leadership Computing Facility’s Frontier supercomputer [30] and set a time limit of two hours (Max Walltime for single node reservation on Frontier) to determine the maximum size of the HHL circuit that can be generated within this constraint. For each execution, we set timers for each component of the HHL circuit generation procedure, including time consumption of QPE and inverse QPE circuits, summation of various other components of HHL circuit since they take less than 1% of the entire computation, and to save the circuit in a qpy format file (a binary serialization format integrated in Qiskit for `QuantumCircuit` and `ScheduleBlock`

Table 1: Comparative analysis of time consumption, gate count, and circuit depth between standard QPE and LuGo across various matrix sizes.

Matrix Size	Qubits	Standard QPE			LuGo			Reduction		
		Time (s)	Gate	Depth	Time (s)	Gate	Depth	Time	Gate	Depth
$2^1 \times 2^1$	5	0.05	88	72	0.09	56	40	0.51×	1.57×	1.80×
$2^2 \times 2^2$	7	0.16	375	343	0.11	151	119	1.48×	2.48×	2.88×
$2^3 \times 2^3$	9	1.63	3,718	3,672	0.34	722	676	4.86×	5.15×	5.43×
$2^4 \times 2^4$	11	17.37	38,633	38,571	1.34	4,388	4,326	12.95×	8.80×	8.92×
$2^5 \times 2^5$	13	189.26	343,250	343,170	6.50	19,194	19,114	29.13×	17.88×	17.95×
$2^6 \times 2^6$	15	1908.18	2,876,007	2,875,907	37.65	91,054	90,954	50.68×	31.59×	31.62×
$2^7 \times 2^7$	17	Timeout	Timeout	Timeout	148.27	416,462	416,340	N/A	N/A	N/A
$2^8 \times 2^8$	19	Timeout	Timeout	Timeout	643.42	1,866,991	1,866,845	N/A	N/A	N/A
$2^9 \times 2^9$	21	Timeout	Timeout	Timeout	3287.47	8,257,810	8,257,638	N/A	N/A	N/A

objects). These measurements provide detailed insights into the time consumption of each process. Finally, we use Qiskit’s AerSimulator (version 0.16.0) to simulate the generated HHL circuits for validating the accuracy of LuGo, by comparing the fidelity of the results obtained using LuGo with that from the standard QPE implementation.

The evaluation is primarily focused on two metrics: execution time and circuit statistics, including gate count and circuit depth. Figure 1 illustrates the time consumption statistics associated with generating HHL circuits using LuGo compared to the standard QPE method. Figure 1a shows the time consumption of generating QPE circuits with respect to the size of unitary matrix input. Figure 1b presents a logarithmic scale plot of the time required for generating both QPE and inverted QPE circuits, which account for over 99% of the total circuit generation time. Figure 1c details the time consumption involved in generating other components of HHL circuits. These include the HHL circuits’ components such as state preparation, eigenvalue reciprocal computation, and controlled rotation circuits. Figure 1d depicts the time required to save the circuits in a qpy format file. LuGo demonstrates advantages over standard QPE due to its lower memory storage requirements and more efficient input/output writing processes because of a compact controlled unitary circuit generation approach.

Figure 1 also shows that plots of the LuGo results have a significantly lower slope than the standard QPE method, indicating superior computational efficiency in circuit generation using LuGo. The slopes of the results in Figures 1a and 1b are similar, which are 0.75 for LuGo and 1.01 for standard QPE. The slope for other components of LuGo is 0.25 while the slope for standard QPE is 0.74. As for saving the generated circuit to storage, the slope for LuGo is 0.41, and for standard QPE is 0.90.

Figure 2 depicts circuit statistics, including total gate count and circuit depth, to generate HHL circuits. LuGo achieves less gate and circuit depth requirement compared with the standard QPE generation approach. LuGo obtained around $1.5\times$ to $2\times$ gate counts and circuit depth reduction for a 2×2 matrix input and over $30\times$ gate and circuit depth reduction over standard QPE for the largest system of equations tested, demonstrating better scalability over standard QPE approach.

Table 1 provides the numeric results of comparing the total time consumption and circuit statistics of generating HHL circuits using the standard QPE circuit generation design and the LuGo framework. The first column indicates the size of the matrix input. It is important to note that the matrix input will always be padded to achieve dimensions of $2^n \times 2^n$ for computational purposes. The second column indicate the total number of qubits required for the HHL circuit. This adjustment ensures compatibility with the requirements of the HHL algorithm, which necessitates matrices of this form. The second through fourth columns display the time consumption and circuit statistics, specifically total gates and circuit depth, using a standard QPE generation method. Columns five to seven detail the time consumption and corresponding circuit statistics using LuGo. The time consumption is the minimum time amongst the single-thread and multithreaded LuGo implementation, later discussed in Figure 3. Finally, the last three columns illustrate the enhancement achieved by LuGo over a standard QPE implementation in terms of time, gate count, and circuit depth.

The HHL circuit generation algorithm using standard QPE can generate HHL circuits with matrix sizes from $2^1 \times 2^1$ to $2^6 \times 2^6$ within two hours using one node of the Frontier supercomputer. Note that the standard QPE implementation is not parallelized. Whereas the LuGo framework can generate circuits for matrix sizes up to $2^9 \times 2^9$, which is a $64\times$ matrix size scalability compared to the existing approach for the given time limit. As for gate counts and circuit depth, LuGo achieves gate count reduction over the standard QPE method from $1.57\times$ with matrix size 2×2 to over $30\times$ with matrix size $2^6 \times 2^6$, demonstrating higher scalability on time consumption and circuit statistics.

As discussed in Section 3.2, the generation of HHL circuit requires both QPE and inversed QPE circuits. Traditionally, the generation of a inversed circuit is to simply reverse the order of the circuits and take the inverse operation of each gate of the original circuit. However, such methods are not optimized for multi-threading process. For computations

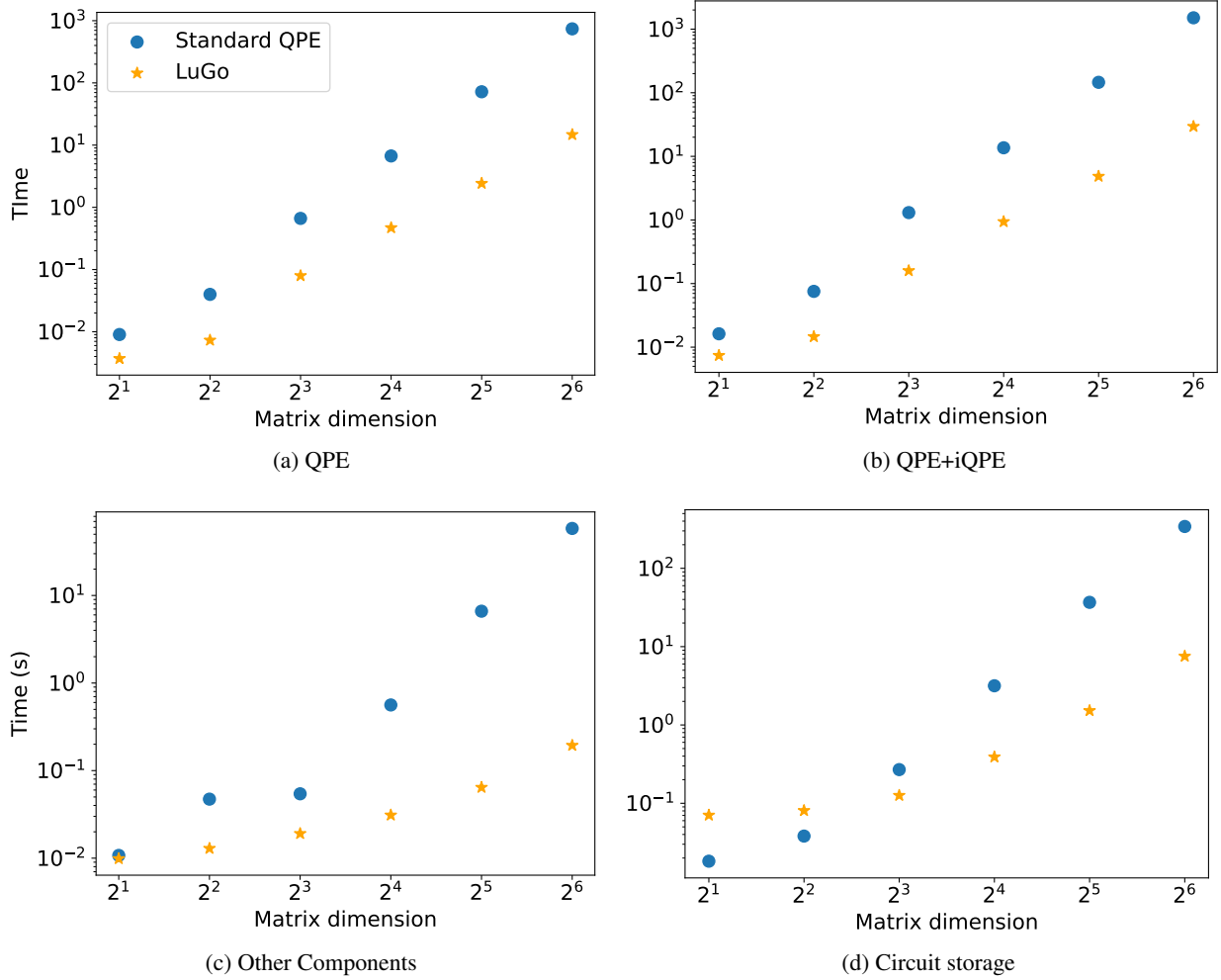


Figure 1: Time to generate HHL circuits using standard QPE and LuGo with single thread version. LuGo demonstrates advantages on circuit generation of QPE and inverse QPE, Other components of QPE circuits, and circuit storage in most of the scenarios.

that requires both QPE and inversed QPE circuit computation, we parallelized the computation of inversed QPE by generating both unitary and inversed unitary circuits to improve the overall performance.

Figure 3 illustrates the comparison of time consumption between the single-threaded and multithreaded versions of the LuGo framework. The number of threads used by LuGo equals to the number of clock qubits. The initialization of the Python multithreading package `ray` introduces additional overhead, causing all test cases to exceed 10 seconds for completion. Thus, for matrices with dimensions up to $2^6 \times 2^6$, the single-threaded version demonstrates superior performance since it avoids the overhead associated with initializing the multithreading package. However, for matrix sizes exceeding $2^6 \times 2^6$, the multithreaded version of LuGo outperforms its single-threaded counterpart. For matrix size of $2^9 \times 2^9$, LuGo multithreaded version takes 3287.47 seconds, and single-thread version requires 5504.17 seconds to perform the task, which is a $1.67\times$ reduction on time consumption using the multithreaded version.

We also compare the fidelity results of LuGo against the standard QPE across varying tridiagonal Toeplitz matrix sizes ranging from $2^1 \times 2^1$ to $2^6 \times 2^6$. The circuits are run using an ideal quantum simulator, Qiskit’s `AerSimulator`, with 1,000,000 shots for each circuit for 50 repetitions. The results are averaged for each test case to eliminate randomness of each simulation run. The results in Figure 4 demonstrate remarkable consistency in performance between both approaches, with all computed fidelity exceeding 0.998 across the tested matrix sizes. Notably, there is no discernible difference in the fidelity outcomes between LuGo and standard QPE, highlighting the robustness and reliability of LuGo. This similarity in performance underscores the validity of LuGo as an effective alternative to the standard QPE for phase estimation tasks, even as the complexity of the problem increases.

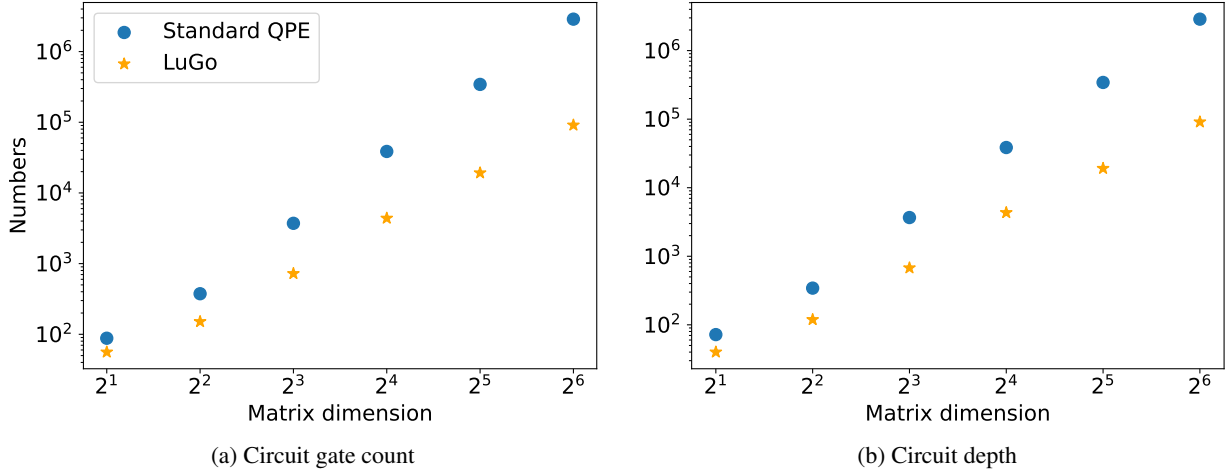


Figure 2: Circuits statistics comparison of standard QPE and LuGo to generate HHL circuits. From the two figures, LuGo reduced quantum gates and circuit depth requirement to generate HHL circuits exponentially, providing better scalability over standard QPE generation method.

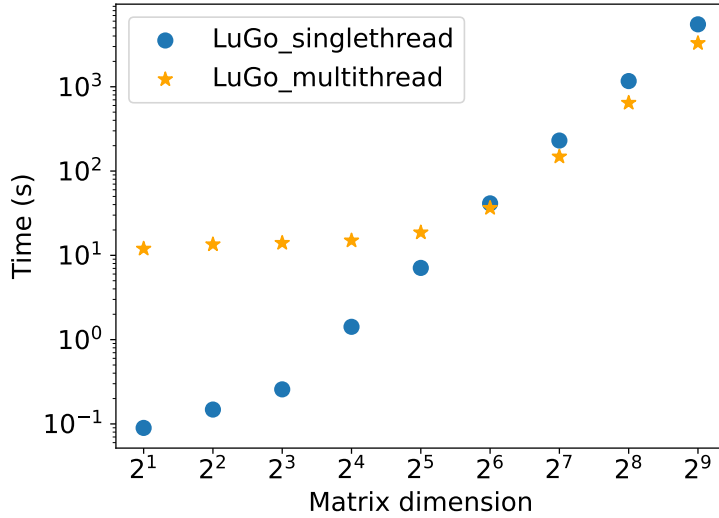


Figure 3: Time consumption for generating HHL circuits using LuGo. Single threaded LuGo has better performance on matrix dimension less than $2^6 \times 2^6$ and multithreaded LuGo spent less on matrices larger than $2^7 \times 2^7$.

3 Methods

3.1 Quantum Phase Estimation

QPE is designed to estimate the phase $|\lambda\rangle$ associated with an eigenvector $|\phi\rangle$ of a unitary operator U . Figure 5 and Figure 6 depicts the overall circuit and generation method to perform QPE. The circuit consists of two main registers: the clock register and the input qubits. Initially, the clock register, composed of k qubits, is set to the state $|0\rangle$. A Hadamard gate is applied to each qubit in this register, transforming it into a superposition state $\frac{1}{\sqrt{2^n}} \sum_{k=0}^{2^n-1} |k\rangle$, which prepares the clock qubits for phase estimation.

Following the Hadamard operations, controlled-unitary ($c-U$) gates are applied. Each clock qubit controls a U raised to an exponentially increasing power—specifically, the t -th qubit controls $U^{2^{t-1}}$. The novelty of our LuGo implementation is to address this exponentially increasing computation of the controlled-unitary operations, as elaborated

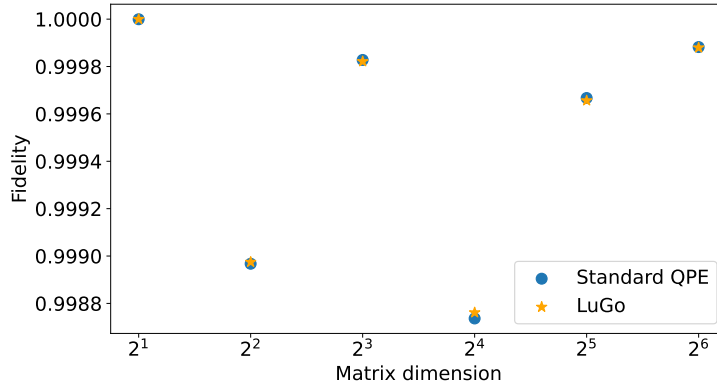


Figure 4: Fidelity comparison of tridiagonal Toeplitz linear systems of equations. Fidelity is defined by the difference between the classical linear solver solution (numpy linear solver Python package) and the quantum solution using the HHL algorithm. A fidelity of 1 means no difference, while a low score close to 0 suggest discrepancies between the estimated and true values.

in Section 3.3. This sequence of operations entangles the clock register with the input state $|\phi\rangle$, encoding the phase

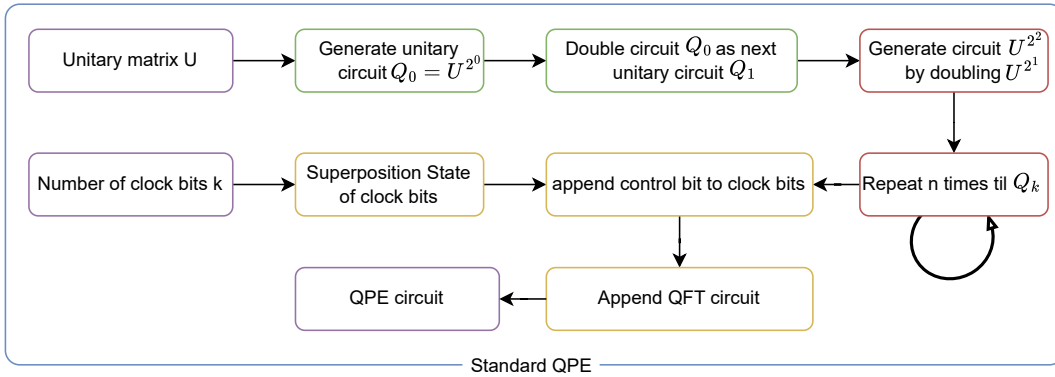


Figure 5: Standard QPE circuit generation process.

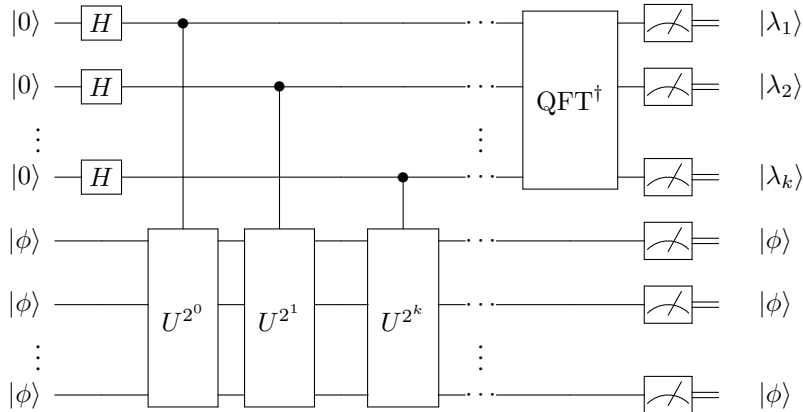


Figure 6: QPE circuit to estimate phase of input u . The QPE algorithm will estimate the state of $|u\rangle$ and generate eigenvalues λ of matrix u

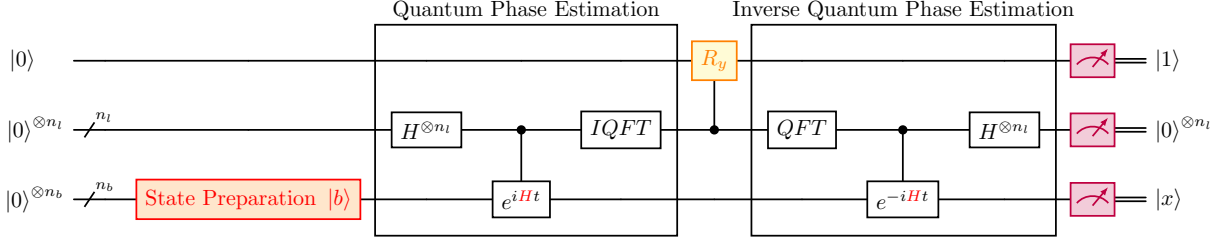


Figure 7: Quantum circuit for the HHL algorithm. The circuit includes the QPE part, eigenvalue reciprocal part, the conditional rotation part, and the inverse QPE part. Measurement of the ancilla qubit determines the success of the algorithm.

ϕ into the clock qubits through the mechanism known as “phase kickback”. As a result, the combined state becomes $\frac{1}{\sqrt{2^n}} \sum_{k=0}^{2^n-1} e^{2\pi i k \theta} |k\rangle |\phi\rangle$.

To decode this encoded phase information, an inverse Quantum Fourier Transform (QFT) is applied to the clock register. This transformation converts the superposition state into a binary representation of $|\lambda\rangle$, enabling us to measure the clock qubits and obtain an estimate of $|\lambda\rangle$ with high precision. Equation 1 depicts the overall procedure:

$$\left(\frac{1}{\sqrt{2^n}} \sum_{k=0}^{2^n-1} |k\rangle \otimes |\phi\rangle \right) \xrightarrow{c-U} \frac{1}{\sqrt{2^n}} \sum_{k=0}^{2^n-1} e^{2\pi i \lambda} |k\rangle \otimes |\phi\rangle \xrightarrow{QFT^\dagger} |k\rangle \otimes |\phi\rangle. \quad (1)$$

Throughout these operations, the input state $|\phi\rangle$ remains unchanged except for acquiring the phase factor $e^{2\pi i \lambda}$, ensuring that it is preserved for potential further use in subsequent quantum computations.

To design the controlled unitary operations for QPE circuits, an algorithm that encode the unitary circuits to the corresponding quantum circuits is required. The default circuit generation approach in Qiskit (version 1.3) utilizes the Peter–Weyl decomposition algorithm [31–33]. This approach is particularly efficient for designing unitary operators with symmetries or in scenarios where the target unitary arises naturally from group-theoretic considerations. It produces a more compact circuit compared with the Trotterization method as it trims out redundant computation for accurate unitary circuits output.

3.2 Harrow–Hassidim–Lloyd Algorithm

The Harrow–Hassidim–Lloyd (HHL) algorithm is a canonical quantum algorithm to solve linear systems of equations [29]. It is one of the quantum algorithms that shows exponential acceleration over classical computation that utilizes QPE as a sub-algorithm for the computation. For the overall computational scheme for the HHL algorithm to solve a linear system of an equation $A\vec{x} = \vec{b}$, three parts are required: QPE, reciprocal of eigenvalues, and inverse QPE, as shown in Figure 7. In order to convert a matrix to a unitary matrix for QPE implementation, the input matrix A is initialized as a series of controlled-unitary gates, e^{iH2^t} , where H is the input matrix A if it is Hermitian. If the matrix A is not Hermitian, it can be padded and converted to a Hermitian $H = \begin{bmatrix} A & 0 \\ 0 & A^\dagger \end{bmatrix}$, and the vector b can be

initialized as $c = \begin{bmatrix} 0 \\ b \end{bmatrix}$ to match matrix H . Then, the unitary matrix e^{iH2^t} is computed by a unitary circuits generation algorithm. By default in Qiskit, the unitary circuits generation algorithm is performed using the Peter–Weyl decomposition to generate each controlled-unitary circuit [31–33]. After these circuits are generated, the algorithm constructs reciprocal eigenvalue circuits. Finally, it integrates the controlled-unitary gates with other components of the HHL circuit to complete the circuit generation process.

3.3 LuGo: a scalable and efficient implementation for QPE circuits

Generation of the QPE circuit predominantly consumes time during the creation of the controlled-unitary circuit, particularly in the repetition of controlled-unitary operations for U^{2^n} . Therefore, reducing the time required for these controlled-unitary operations is crucial to minimizing both circuit depth and overall computation time. In standard QPE implementations, quantum circuits for the controlled-unitary operation $U = e^{iH2^t}$ (where $t = 1, 2, 3, \dots, k$) are designed by first constructing the initial controlled-unitary circuit for e^{iH} using the Peter–Weyl decomposition method.

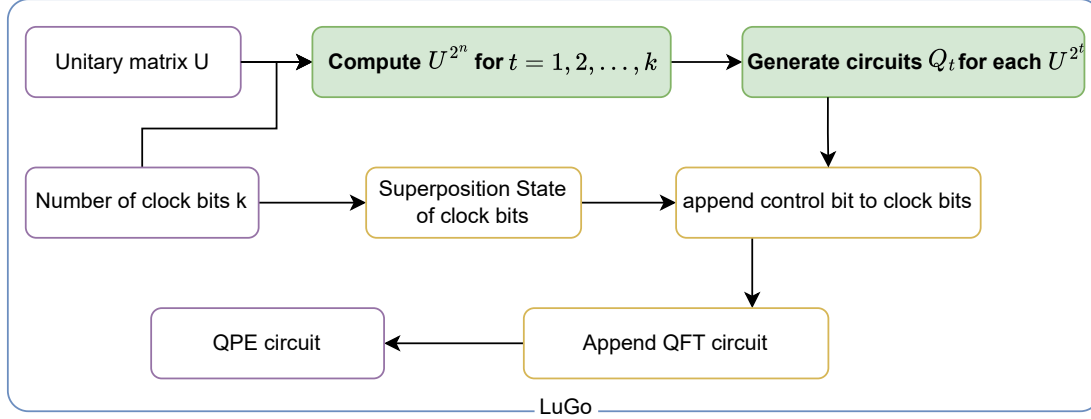


Figure 8: Proposed LuGo designing process. We highlight the operation that obtained acceleration over standard QPE.

Algorithm 1 LuGo framework for QPE.

Input: Hermitian matrix input H , vector input $|\phi\rangle$, and k clock qubits.

Output: QPE circuit available to execute on quantum hardware.

- 1: **for** $t \leftarrow (0 \text{ to } k)$ **do in parallel**
 - 2: Compute and store unitary matrix e^{iH2^t} as U_t .
 - 3: Generate controlled unitary circuit Q_t based on U_t .
 - 4: **end for**
 - 5: Initialize the clock qubits $|k\rangle$ using Hadamard gates.
 - 6: Prepare the quantum State $|\phi\rangle$ at input qubits.
 - 7: Append each Q_t to input qubits and clock qubits.
 - 8: Append $iQFT$ circuit to clock qubits.
 - 9: **return** Generated QPE circuit.
-

Subsequent circuits for e^{iH2^t} are created by replicating this initial circuit. This process results in the generated first unitary circuit being repeated $2^k - 1$ times, where k denotes the number of clock qubits. However, as the number of clock qubits increases linearly with the qubit count, the repetition of controlled-unitary gates grows exponentially. Consequently, this exponential increase significantly affects both the circuit generation time and the total gate count required, particularly as the system scales to larger qubit sizes.

To address these challenges, we introduce a new approach, namely LuGo, to enhance QPE circuit design and reduce circuit depth without sacrificing fidelity. Our methodology focuses on optimizing the design and execution of QPE by improving the controlled-unitary matrix design efficiency. Figure 8 introduces our LuGo framework. Within this framework, unitary circuits for each component are independently generated using Peter–Weyl decomposition. This approach enhances computational efficiency by minimizing repetition and redundancy when generating the controlled unitary circuits, thereby reducing both the design and execution workload.

To generate the QPE circuits, LuGo enables the parallel computation of controlled-unitary circuits generation shown in Algorithm 1, which is the heaviest part for QPE circuits generation. Firstly, the QPE circuit takes the Hermitian matrix H , input vector $|\phi\rangle$, and number of clock qubits k . Once all inputs are fed into the algorithm, the algorithm will first perform the parallel computation for controlled-unitary circuits generation (Lines 1–4). Once the generation of each controlled-unitary circuit finishes, rest of the procedure is to assemble the components of QPE circuits together by first appending Hadamard gates to clock qubits to initialize clock qubits (Line 5). Next, a quantum state preparation algorithm is performed to initialize quantum state $|\phi\rangle$ (Line 6). Then, the algorithm will assign each controlled-unitary circuit to clock qubits and input qubits (Line 7). After the inversed QFT circuits are appended to the circuits (Line 8), the algorithm returns the generated QPE circuit as the output (Line 9).

By employing the classical matrix exponentiation algorithm [34], each controlled-unitary circuit is generated independently. This independence allows for the distribution of computational tasks across multiple processing units, enabling efficient parallel computation. The number of clock qubits determines the maximum number of CPU cores required

by LuGo. Consequently, the time required to construct the QPE circuit is significantly reduced, as different segments of the circuit can be generated simultaneously without sequential dependencies.

For scenarios when designing controlled-unitary circuits for specific unitary matrices is challenging for certain unitary circuits generation algorithm, a hybrid approach is imported for unitary operator computation. This approach distributes the computation of controlled-unitary operators across both classical and quantum resources to achieve optimal efficiency and robustness. By leveraging the flexibility of hybrid computation, this method ensures compatibility and scalability for generating complex unitary operators, enabling efficient and reliable HHL circuit design.

3.4 Complexity analysis

The number of qubits used for the QPE circuit generation will remain unchanged between the standard QPE and LuGo implementations. The total number of qubits required for a QPE circuit is $n + k$, where k is the clock qubits and n input qubits. The number of clock qubits can be written as $k = \mathcal{O}(\log(1/\epsilon))$, where ϵ is the precision of the QPE algorithm. For quantum gate complexity, the standard QPE requires the design of the first controlled-unitary circuit and repeat 2^k times for computation of U^{2^k} . Assume the design of the first controlled unitary circuit with complexity of $\mathcal{C}(U)$, and the gates complexity of inserting a inverse QFT circuit is $\mathcal{O}(k \cdot \log k)$ for the optimized approach. Notice that the complexity of QFT is much less than the controlled unitary gates, the gate complexity of a standard QPE is $\mathcal{O}(2^k \mathcal{C}(U))$.

Since all the components mentioned above is sequential for QPE circuit, the circuit depth complexity is similar to the gate complexity, which is $\mathcal{O}(2^k \mathcal{D}(U))$, where $\mathcal{D}(U)$ denotes the depth complexity of the generated controlled-unitary circuit. For LuGo, the controlled-unitary circuit is generated independently, which means it is not formed by the repetition of the first controlled-unitary gate. Therefore, QPE circuit generation process does not require exponential stacking of controlled-unitary gates. The gate complexity of LuGo, therefore, is $\mathcal{O}(k \mathcal{C}(U))$. Thus, the generation of quantum circuits are throttled on memory consumption, where it is related to the number of qubits and numbers of quantum gates.

The LuGo algorithm introduced here offers significant advantages by reducing overall computation time. The computation of e^{iH2^t} is optimized using an efficient matrix exponential algorithm on classical computer, which reduces computational overhead on the quantum side [34]. Classical computation for matrix exponentiation by squaring, a well-studied approach, has a time complexity of $\mathcal{O}(\log n)$ with respect to the exponent indexes, making it far more efficient than the linear stack of controlled-unitary circuits on the standard QPE side. This optimization results in substantial reductions in both time and gate count for QPE circuit generation.

4 Discussion and Conclusion

We introduce the LuGo algorithm that enhances the performance of Quantum Phase Estimation (QPE) by reducing the time to generate the circuit with a more compact QPE circuit design. The QPE circuit generated by LuGo can apply on any quantum circuits that utilize QPE circuit. We demonstrate the capability of LuGo by generating circuits for a quantum linear systems algorithm, the HHL algorithm. The LuGo algorithm achieves $50.68\times$ reduction on time consumption and over $31\times$ on quantum gates and circuit depth reduction to solve a system of linear equations with a matrix size of $2^6 \times 2^6$. LuGo can generate HHL circuits for solving a matrix size of $2^9 \times 2^9$ within one hour on the Frontier supercomputer, which is a $64\times$ scalability on matrix size over the standard QPE approach. By simulating the generated linear solver circuits, LuGo obtained almost identical fidelity compared to standard QPE circuit generation method.

Our LuGo framework demonstrates better scalability on time consumption and gate count and circuit depth over the existing approach. With the tremendous efficiency improvement of QPE circuit generation, LuGo achieve one more step towards real-world applications of quantum computing. Despite that the paper demonstrates solving linear systems of equations using tridiagonal Toeplitz matrices, LuGo can be applied on any arbitrary linear systems without any adjustments of the LuGo framework.

However, the scalability of the QPE algorithm is still limited due to heavy computation overhead and repetition of controlled-unitary circuits with number of clock qubits. The controlled-unitary circuits highly rely on unitary circuits generation algorithms, which still lack scalability and limits the performance of QPE circuits generation algorithm. Therefore, it is still crucial to improve the controlled-unitary circuits generation algorithms for fewer gates and time consumption while maintaining high fidelity for the efficient QPE computation.

Acknowledgement

This research used resources of the Oak Ridge Leadership Computing Facility at the Oak Ridge National Laboratory, which is supported by the Office of Science of the U.S. Department of Energy under Contract No. DE-AC05-00OR22725. The authors sincerely appreciate the insightful discussions and feedback from Alessandro Baroni, Seongmin Kim, Antigoni Georgiadou, In-Saeng Suh, Tom Beck, and Travis Humble.

Data and code availability

Correspondence and requests for material should be addressed to Chao Lu and Muralikrishnan Gopalakrishnan Meena. Our codes are available for academic or commercial use. Please reach out to the authors or luc1@ornl.gov, gopalakrishm@ornl.gov.

References

- [1] IBM Research, “Qiskit: Open-Source Quantum Development,” Accessed: March 2022. [Online]. Available: <https://qiskit.org>.
- [2] R. Acharya, L. Aghababaie-Beni, I. Aleiner, T. Andersen, M. Ansmann, F. Arute, K. Arya, A. Asfaw, N. Astrakhantsev, J. Atalaya *et al.*, “Quantum error correction below the surface code threshold (2024),” *arXiv preprint arXiv:2408.13687*, 2024.
- [3] R. Kharsa, A. Bouridane, and A. Amira, “Advances in quantum machine learning and deep learning for image classification: a survey,” *Neurocomputing*, vol. 560, p. 126843, 2023.
- [4] W. Li, C.-h. Wang, G. Cheng, and Q. Song, “International conference on machine learning,” *Transactions on machine learning research*, 2023.
- [5] R. Di Sipio, J.-H. Huang, S. Y.-C. Chen, S. Mangini, and M. Worring, “The dawn of quantum natural language processing,” in *ICASSP 2022-2022 IEEE International Conference on Acoustics, Speech and Signal Processing (ICASSP)*. IEEE, 2022, pp. 8612–8616.
- [6] T. Monz *et al.*, “Realization of a Scalable Shor Algorithm,” *Science*, vol. 351, no. 6277, pp. 1068–1070, 2016.
- [7] R. Weiss, A. Baroni, J. Carlson, and I. Stetcu, “Reaction dynamics with qubit-efficient momentum-space mapping,” *arXiv preprint arXiv:2404.00202*, 2024.
- [8] M. Gopalakrishnan Meena, K. C. Gottiparthi, J. G. Lietz, A. Georgiadou, and E. A. Coello Pérez, “Solving the hele–shaw flow using the harrow–hassidim–lloyd algorithm on superconducting devices: A study of efficiency and challenges,” *Physics of Fluids*, vol. 36, no. 10, 2024.
- [9] L. Lapworth, “A hybrid quantum-classical cfd methodology with benchmark hhl solutions,” *arXiv preprint arXiv:2206.00419*, 2022.
- [10] C.-C. Ye, N.-B. An, T.-Y. Ma, M.-H. Dou, W. Bai, D.-J. Sun, Z.-Y. Chen, and G.-P. Guo, “A hybrid quantum-classical framework for computational fluid dynamics,” *Physics of Fluids*, vol. 36, no. 12, 2024.
- [11] I. Y. Dodin and E. A. Startsev, “On applications of quantum computing to plasma simulations,” *Physics of Plasmas*, vol. 28, no. 9, 2021.
- [12] M. A. Nielsen and I. L. Chuang, *Quantum computation and quantum information*. Cambridge university press, 2010.
- [13] A. Montanaro, “Quantum algorithms: an overview,” *npj Quantum Information*, vol. 2, no. 1, pp. 1–8, 2016.
- [14] A. Y. Kitaev, “Quantum measurements and the abelian stabilizer problem,” *arXiv preprint quant-ph/9511026*, 1995.
- [15] C. Developers, *Cirq*. Zenodo, May 2024. [Online]. Available: <https://zenodo.org/doi/10.5281/zenodo.4062499>
- [16] V. Bergholm, J. Izaac, M. Schuld, C. Gogolin, S. Ahmed, V. Ajith, M. S. Alam, G. Alonso-Linaje, B. Akash-Narayanan, A. Asadi *et al.*, “Pennylane: Automatic differentiation of hybrid quantum-classical computations,” *arXiv preprint arXiv:1811.04968*, 2018.
- [17] J.-S. Kim, A. McCaskey, B. Heim, M. Modani, S. Stanwyck, and T. Costa, “Cuda quantum: The platform for integrated quantum-classical computing,” in *2023 60th ACM/IEEE Design Automation Conference (DAC)*. IEEE, 2023, pp. 1–4.
- [18] A. W. Services, “Amazon Braket,” 2020. [Online]. Available: <https://aws.amazon.com/braket/>

- [19] A. Daspal and A. F. Izmaylov, “Minimizing trotter approximation error in quantum phase estimation using genetic algorithm,” in *2024 IEEE International Conference on Quantum Computing and Engineering (QCE)*, vol. 2. IEEE, 2024, pp. 520–521.
- [20] C. Kang, N. P. Bauman, S. Krishnamoorthy, and K. Kowalski, “Optimized quantum phase estimation for simulating electronic states in various energy regimes,” *Journal of Chemical Theory and Computation*, vol. 18, no. 11, pp. 6567–6576, 2022.
- [21] H. Ni, H. Li, and L. Ying, “On low-depth algorithms for quantum phase estimation,” *Quantum*, vol. 7, p. 1165, 2023.
- [22] J. G. Smith, C. H. Barnes, and D. R. Arvidsson-Shukur, “Iterative quantum-phase-estimation protocol for shallow circuits,” *Physical Review A*, vol. 106, no. 6, p. 062615, 2022.
- [23] E. van den Berg, “Iterative quantum phase estimation with optimized sample complexity,” in *2020 IEEE International Conference on Quantum Computing and Engineering (QCE)*. IEEE, 2020, pp. 1–10.
- [24] J. Li, “Iterative method to improve the precision of the quantum-phase-estimation algorithm,” *Physical Review A*, vol. 109, no. 3, p. 032606, 2024.
- [25] H. Mohammadbagherpoor, Y.-H. Oh, P. Dreher, A. Singh, X. Yu, and A. J. Rindos, “An improved implementation approach for quantum phase estimation on quantum computers,” in *2019 IEEE International Conference on Rebooting Computing (ICRC)*. IEEE, 2019, pp. 1–9.
- [26] S. Johnstun and J.-F. Van Huele, “Optimizing the phase estimation algorithm applied to the quantum simulation of heisenberg-type hamiltonians,” *arXiv preprint arXiv:2105.05018*, 2021.
- [27] P. Rall, “Faster coherent quantum algorithms for phase, energy, and amplitude estimation,” *Quantum*, vol. 5, p. 566, 2021.
- [28] Y. Dong, J. A. Gross, and M. Y. Niu, “Optimal low-depth quantum signal-processing phase estimation,” *arXiv preprint arXiv:2407.01583*, 2024.
- [29] A. W. Harrow, A. Hassidim, and S. Lloyd, “Quantum algorithm for linear systems of equations,” *Physical Review Letters*, vol. 103, no. 15, Oct. 2009. [Online]. Available: <http://dx.doi.org/10.1103/PhysRevLett.103.150502>
- [30] S. Atchley, C. Zimmer, J. Lange, D. Bernholdt, V. Melesse Vergara, T. Beck, M. Brim, R. Budiardja, S. Chandrasekaran, M. Eisenbach *et al.*, “Frontier: exploring exascale,” in *Proceedings of the International Conference for High Performance Computing, Networking, Storage and Analysis*, 2023, pp. 1–16.
- [31] A. W. Cross, L. S. Bishop, S. Sheldon, P. D. Nation, and J. M. Gambetta, “Validating quantum computers using randomized model circuits,” *Physical Review A*, vol. 100, no. 3, p. 032328, 2019.
- [32] B. Kraus and J. I. Cirac, “Optimal creation of entanglement using a two-qubit gate,” *Physical Review A*, vol. 63, no. 6, p. 062309, 2001.
- [33] B. Drury and P. Love, “Constructive quantum shannon decomposition from cartan involutions,” *Journal of Physics A: Mathematical and Theoretical*, vol. 41, no. 39, p. 395305, 2008.
- [34] A. H. Al-Mohy and N. J. Higham, “A new scaling and squaring algorithm for the matrix exponential,” *SIAM Journal on Matrix Analysis and Applications*, vol. 31, no. 3, pp. 970–989, 2010.